**ORIGINAL PAPER**

# Irradiation Creep - Swelling Interaction in Modified 316 Stainless Steel up to 200 dpa

Shigeharu Ukai* and Satoshi Ohtsuka**

** Hokkaido university, N13, W8, Kita-ku, Sapporo, 060-8628*

*** Japan Atomic Energy Agency, 4002, Narita, Oarai-machi, Higashi-ibaraki-gun, Ibaraki 311-1393, Japan*

The irradiation creep–swelling interaction parameters were precisely derived for Monju fuel pin cladding PNC316 by irradiation tests of pressurized tubes in FFTF. It was found out that creep-swelling coupling coefficient decreased and asymptotically approached a constant value as the swelling progresses, although it was widely believed that irradiation creep rate could be proportional to the swelling rate. This non-proportionality in the irradiation creep-swelling interaction was investigated by means of the rate theory analyses under sequential climb-controlled glide process of dislocation due to absorption of interstitial atoms. It was clarified through a constructed robust model that the presence of a precipitate sink should upset the proportionality of the net interstitial flux into dislocations to the net vacancy flux into the voids. In addition, irradiation creep parameters derived by material irradiation was demonstrated to be applicable for predicting the irradiation creep deformation in the fuel pins.

***KEYWORDS:*** *irradiation creep, irradiation creep-swelling interaction, PNC316, climb-controlled glide process of dislocation, precipitate sink, void sink, dislocation sink*

Corresponding author, E-mail: s-ukai@eng.hokudai.ac.jp

## I. Introduction

Irradiation creep deformation of stainless steels has been studied in a great concern of reactor design for more than three decades. It was consistently shown that the irradiation creep rate is the sum of two terms, one independent of swelling and one strongly coupled with the swelling rate. The major components of the instantaneous creep rate can be expressed by the following empirical equation[1,2]:

$$\dot{\varepsilon} / \sigma = B_0 + D \cdot \dot{S} \quad . \qquad \text{--------} \quad (1)$$

where $\dot{\varepsilon}$ is instantaneous irradiation creep rate, $\sigma$ is effective stress, $B_o$ is the creep compliance, D is the irradiation creep-swelling coupling coefficient, and $\dot{S}$ is the instantaneous volumetric swelling rate per dpa.

Irradiation creep has been studied by the irradiation of pressurized tubes. Based on the most extensive review by Garner[3], Bo of austenitic stainless steels is typically in the range from 0.5 to 4 $x10^{-6}$ $MPa^{-1}$ $dpa^{-1}$. It was also shown in the previous study that Bo ranges from 0.4 to 1.2 $x10^{-6}$ $MPa^{-1}$ $dpa^{-1}$ for modified 316 stainless steel[4], which was developed for the Prototype Fast Breeder Reactor MONJU cladding in Japan Atomic Energy Agency (JAEA) and was designated PNC316 [5,6]. This swelling independent term has been well interpreted in terms of the stress-induced preferential absorption (SIPA) mechanism under active investigations for many years. The SIPA mechanism proposed by Heald and Speight[7], Wolfer and Ashkin[8], and Bullough and Willis[9] depends solely on differences in the climb rate of dislocations whose orientation relative to the applied stress influences their absorption of point defects. Dislocations with their Burgers vector parallel to the external stress direction can more easily absorb

interstitial atoms and can take climb motion than those with their Burgers vector perpendicular to the external stress. Thus, SIPA produces a stress-induced bias differential among dislocations, causing anisotropic dislocation climb and loop growth, which leads to the total deviatoric strain along the external stress. This creep mechanism provides the best opportunity to explain many of the irradiation creep observations under condition where swelling is not significant.

Concerning irradiation creep driven by swelling, Gittus firstly proposed the I-creep model to account for coupling between irradiation creep and swelling[10]. In this model, irradiation creep is induced by sequential climb-glide process of dislocation due to absorption of interstitial atoms under dislocation bias, whilst excess vacancies produce voids. Therefore, this mechanism predicts an irradiation creep rate proportional to swelling rate[11], which means that the D value turns out to be constant according to equation (1). The value of D derived from irradiation tests using the pressurized tubes of austenitic stainless steels is very limited, and results of around $2 \times 10^{-3}$ $MPa^{-1}$ are reported from CEA for 316Ti and 1515Ti[12] and PNC316[4]. These values of D were derived from the integral form of equation (1), assuming constant stress and constant temperature with respect to neutron dose. Garner suggested that this D value approached $6 \times 10^{-3}$ $MPa^{-1}$ if the instantaneous swelling rate is taken into account[3]. In addition, Toloczko and Garner pointed out an effect of stress that leads to an enhancement of swelling itself[13].

In this study, the creep-swelling coupling coefficient D is more precisely investigated. The instantaneous irradiation creep rate of PNC316 was derived from the results of a pressurized tube experiment using Material Open Test Assembly (MOTA) in Fast Flux Test Facility (FFTF) as well as a fuel pin irradiation in FFTF. A rate theory

model was applied and a new interpretation was proposed for the characteristic feature of irradiation creep-swelling interaction.

## II. Experiment

### 1. Materials irradiation tests

(1) Experimental procedure

The pressurized tube irradiation tests were conducted using the 55MK heat of PNC316. The chemical composition of 55MK heat is listed in **Table 1**. In PNC316, minor elements titanium, niobium, phosphorus and boron are added within the specification of Japan Industrial Standard of 316 stainless steel. The 20% cold-working condition was provided after the solution treatment at 1353 K for 2 min. The irradiation creep specimens were cut from the cladding segments of the 55MK heat with a dimension of 6.5 mm diameter and 0.47 mm thickness. End caps were electron beam welded to the specimens. After gas filling with helium to the pressure required to produce the desired stress at the intended irradiation temperature, the specimens were sealed by laser welding of the fill hole located in the specimen top end cap.

Table 1

The pressurized tubes and open tubes of 28.1 mm length were irradiated using the MOTA irradiation vehicle at FFTF[14]. The temperature, hoop stress, neutron dose, final diameter changes and FFTF irradiation cycles for each specimen are given in **Table 2**. Six irradiation temperatures were selected: 678 K, 713 K, 768 K, 823 K, 878 K and 943 K, which were monitored by thermocouples and controlled within an accuracy of ±5 K during irradiation. The hoop stresses were set to 70 and 100 MPa for the pressurized tubes. The neutron dose varied from 70 to 206 dpa, depending on FFTF irradiation cycle as well as the axial position of specimens located in the MOTA

Table 2

vehicle. The outer diameter of pressurized tubes and open tubes were measured non-destructively during the reactor shutdown intervals using a laser profilometer. In addition, the density of both pressurized and open tubes was destructively measured after completion of the irradiation to evaluate the stress enhanced swelling in the pressurized tubes.

(2) Results

The hoop strain due to irradiation creep, $\varepsilon_h$, can be estimated using following equation:

$$\varepsilon_h = (\Delta D / D_o)_t - (\Delta D / D_o)_s, \qquad \text{--------} \quad (2)$$

where $(\Delta D / D_o)_t$ is the diameter change of the pressurized tubes and $(\Delta D / D_o)_s$ is the swelling strain which is determined by diameter changes of the open tubes or one-third of density changes of corresponding pressurized tubes under the condition of negligible thermal creep. The hoop strain was converted to the equivalent strain using the correlation of $\varepsilon = (2/\sqrt{3}) \cdot \varepsilon_h$, whilst swelling strains were directly plotted in hoop strains. The term of creep strain, $\varepsilon$, hereafter means equivalent strain. **Fig.1** shows the creep and swelling strains at 678 K as a function of neutron dose. The profilometry data estimated during the reactor shutdown intervals were already reported in ref. 6. The fitting curves are also shown, which are later used for deriving the instantaneous coupling coefficient D. The swelling strains indicated by open symbols in **Fig.1** were derived from density measurement at the end of the irradiation. The one-third of the density change almost agrees with the result of diameter change for the

Fig.1

open tube, whilst swelling strains from the density measurement of the pressurized tubes at the end of irradiation are slightly enhanced by the stresses of 70 and 100 MPa. The 823 K case is also shown in **Fig.2**[6], where swelling is significantly limited. The irradiation creep data at other temperatures, 713 K, 768 K, 878 K and 943 K, can not be used for analyzing irradiation creep – swelling interaction due to insufficient swelling as shown in **Table 2**.

Fig.2

The irradiation creep strain at the end of irradiation can be expressed by equation (3) which is obtained by integrating equation (1) under the condition of constant stress, constant temperature, constant $B_o$ and D with respect to neutron dose,

$$\varepsilon' / \sigma = B_o \cdot \phi_t' + D \cdot S', \qquad \text{--------} \quad (3)$$

where $\varepsilon'$, $\phi_t'$ and S' are the irradiation creep strain, neutron dose in dpa and volumetric swelling at the end of irradiation. $\sigma$ is equivalent stress, which was converted using the correlation of $\sigma = (\sqrt{3}/2) \cdot \sigma_h$ ($\sigma_h$ =hoop stress). The term of stress, $\sigma$, utilized hereafter also corresponds to equivalent stress. If the data are selected from the negligible swelling region, $B_o$ can be derived as $\varepsilon' / (\sigma \cdot \phi_t')$. The creep compliance $B_o$ for PNC316 turned out to range from 0.4 to $1.2 \times 10^{-6}$ $MPa^{-1}dpa^{-1}$, based on the low dose data at 678 K, 713 K, 768 K and 823 K, where swelling is negligible. The derived values of $B_o$ are shown in **Fig.3**[4]. The irradiation creep-swelling coupling coefficient D was determined as $(\varepsilon' / \sigma - B_o \cdot \phi_t') / S'$. Using the density measurement data at 678 K and 823 K shown by the open symbols at the end of irradiation in **Fig.1** and **Fig.2**, D was derived to be $1.2 - 2.8 \times 10^{-3}$ $MPa^{-1}$. This D value is evaluated as an average over swelling up to the end of irradiation, since

Fig.3

D was regarded as constant for deriving equation (3). In addition, this estimate takes into account the stress enhanced swelling by considering density measurements at completion of irradiation. The detailed results and derivation process are discussed in a previous publication.[4)]

We try to derive the irradiation creep - swelling coupling coefficient D as a function of swelling by directly applying the differential form of equation (1) instead of the integral form of equation (3). Equation (1) can be transformed into following:

$$D = (\dot{\varepsilon} / \sigma - B_o) / \dot{S} \quad . \qquad \text{--------} \quad (4)$$

In order to estimate the instantaneous creep rate and volumetric swelling rate for neutron exposure, fitting curves for both irradiation creep strain and volumetric swelling were derived in terms of the power law type of equation[15)] at 678 K and 823 K, where sufficient swelling was induced to permit evaluating the irradiation creep–swelling interaction. These fitting curves are illustrated in **Fig.1** and **Fig.2**, and shown in equations (5), (6) and (7) for the case of 678 K:

$$S = 3.10 \times 10^{-4} \times (\phi_t - 50)^{2.10}, \qquad \text{--------} \quad (5)$$

$$\varepsilon_{70} = 7.96 \times 10^{-5} \times \phi_t{}^{2.06}, \qquad \text{--------} \quad (6)$$

$$\varepsilon_{100} = 2.12 \times 10^{-4} \times \phi_t{}^{1.91}. \qquad \text{--------} \quad (7)$$

The swelling for equation (5) was estimated by taking three times the swelling strain measured at each reactor operational interval. The neutron exposure is expressed in dpa. The D value can be calculated according to equation (4) by substituting a

differential of equations (5) and (6) or (7). The results of calculating D as a function of volumetric swelling are shown in **Fig.4** and **Fig.5**. As shown in the schematic diagram inserted in **Fig.4**, the irradiation creep term induced by swelling corresponds to D・S・σ. The D value is shown to be higher just at the onset of swelling, and subsequently saturated at an almost constant value. This saturation value is slightly higher than that obtained from the integral equation at the end of irradiation. In particular, higher D value at 100 MPa for 823 K could result from using volumetric swelling obtained from the diametral change of open tubes, which gives a lower estimate than density measurement of the pressurized tube itself which includes stress-enhanced swelling, as shown in **Fig.2**. According to equation (4), a lower swelling prediction leads to an overestime of the D value.

Fig.4

Fig.5

## 2. Fuel pin irradiation tests

(1) Experimental procedure

The fuel pins with PNC316 cladding were irradiated in FFTF as MFA-1 (Monju Fuel Assembly-1)[16]. In this test, 60MK and 60MS heats of PNC316 were employed, for which chemical compositions, solution treatment conditions and cold-work level are shown in **Table 1**. The 169 fuel pins were installed in the fuel assembly. The outer diameter and thickness of cladding are 6.5 mm and 0.47 mm, respectively. The fuel column length is 914 mm. These fuel pins were irradiated at peak linear power of 349 W/cm up to a peak burnup of 147 GWd/t and peak neutron dose of 107 dpa in FFTF.

The outer diameters of fuel pins were measured with a laser profilometer in order to determine the diametral change of cladding due to radiation-induced creep and swelling during post irradiation examination (PIE). Density measurements of cladding were

also conducted to directly determine the swelling, which was subtracted from the total diametral change to give the amount of creep strain. Both diameter and density measurements were conducted for 6 pins in MFA-1.

(2) Results

Typical examples of the measured diametral changes and swelling strains of fuel pins (Pin No.186019) are shown by solid curve and solid circles, respectively in **Fig.6**. The irradiation creep strain corresponds to a difference between these strains. At the distance of about 300 - 500 mm from core bottom, the swelling strains contributed most strongly to the total diametral changes. **Fig.7** shows the measured relationship in total diametral change and swelling strain for six fuel pins. It is clearly shown that the irradiation creep strain is almost constant even with increasing swelling strain, because the difference between the diametral change and swelling strain corresponds to the irradiation creep strain. This finding implies that the irradiation creep strain in fuel pins is dominated by the $B_o$ term and the interaction term with swelling tends to be diminished with increasing swelling. This situation is quantitatively analyzed in the following discussion.

Fig.6

Fig.7

The overall creep modulus, $B_{ov}$, is defined according to equation (1),

$$B_{ov} = B_0 + D \cdot \dot{S}$$

$$= (d\varepsilon / d\phi_t) / \sigma \quad . \qquad \text{--------} \quad (8)$$

The stress, $\sigma$, loading into the cladding tube of a fuel pin is induced by fission gases

accumulated in the fuel pin plenum. The fission gas pressure was calculated by using theoretical volume of fission gases generated in the fuels and empirical release rate of fission gases from the fuels[17]. Fig.8 shows results of calculation on cladding equivalent stress induced by fission gases vs. neutron dose at the distance of 320 mm from core bottom. The cladding stress almost linearly increases with respect of neutron dose, thus following correlation is expressed for cladding loading stress,

Fig.8

$$\sigma = a \phi_t + b \quad , \qquad \text{--------} \quad (9)$$

where a and b are constant. Equation (8) is integrated using equation (9), and the overall creep modulus, $B_{ov}$, can be expressed as:

$$B_{ov} = \varepsilon' / (1/2\, a\, \phi_t'^{\,2} + b\, \phi_t') \quad . \qquad \text{--------} \quad (10)$$

The values of $B_{ov}$ at each axial location in all of pins can be calculated by substituting the measured $\varepsilon'$ and $\phi_t'$ for equation (10). **Fig.9** shows the relation between $B_{ov}$ vs. instantaneous volumetric swelling rate. Based on equation (8), $B_o$ can be estimated when the swelling rate becomes zero in the diagram of $B_{ov}$ vs. $\dot{S}$. The derived range of $B_0$ is 1.1 - 2.8 x $10^{-6}$ $MPa^{-1}dpa^{-1}$ for various PNC316 base fuel pins.

Fig.9

Next, the irradiation creep-swelling coupling coefficient D is estimated, based on equation (1) with the instantaneous swelling rate. The following equation can be derived using equations (8) and (9).

$$d\varepsilon = (B_0 + D\dot{S})(a \phi_t + b)\, d\phi_t \quad . \qquad \text{--------} \quad (11)$$

The following equations are obtained by integrating Equation (11), assuming that D value is an average over swelling up to the end of irradiation.

$$\varepsilon' = B_0 (1/2\, a\, \phi_t'^2 + b\, \phi_t') + a\, D \int \dot{S}\, \phi_t\, d\, \phi_t + b\, D \int \dot{S}\, d\, \phi_t$$

$$= B_0 (1/2\, a\, \phi_t'^2 + b\, \phi_t') + a\, D \int \phi_t\, d\, S + b\, D\, S' . \qquad \text{--------} \quad (12)$$

The second integral part of equation (12) can be expressed by the following equation.

$$\int \phi_t\, d\, S = S'\, \phi_t' - \int S\, d\, \phi_t \quad . \qquad \text{--------} \quad (13)$$

The second term in the right hand side of equation (13) can be integrated in terms of the swelling equation. The creep-swelling coupling coefficient, D, can be consequently determined using the following equation, which was obtained by substituting equation (13) for equation (12):

$$D = \{\varepsilon' - B_0 (1/2\, a\, \phi_t'^2 + b\, \phi_t')\} / [a\, S'\, \phi_t' - a \int S\, d\, \phi_t + b\, S'] . \qquad \text{-----} \quad (14)$$

As previously mention, this D value corresponds to an average over swelling up to the end of irradiation. The values of D derived for PNC316 base fuel pins are shown in **Fig.10**, where the results of six fuel pins are plotted. The swelling-creep coupling coefficient D tends to decline and almost disappear as swelling develops. This reduction of D values as swelling increases accounts for the measured constant creep strain even for increasing swelling as shown in **Fig.7**. From these analyses it is

Fig.10

suggested that the diametric increase of PNC316 fuel pins due to irradiation creep is due mainly to the creep compliance $B_o$ term, and the contribution of the creep-swelling coupling D term is minor in the swelling dominant regime.

In the MOTA irradiation tests with pressurized tubes of PNC316, it was shown that the D values for instantaneous swelling rates rapidly declined with increasing swelling as shown in **Fig.4** and **Fig.5**. This trend of decline in D values is very similar within the range of 1 % swelling. The only difference is that with increasing swelling the D values almost disappear in the case of MFA-1 fuel pins, whilst the D values saturated at a certain level in the case of pressurized tube irradiation in MOTA experiment. This situation could come from the different dislocation structures induced in relation to swelling onset.[3] In MFA-1 fuel pins, the stress loading is relatively low due to the limited amount of the released fission gases at the time of swelling onset, whilst the high stress was always maintained in the MOTA pressurized tubes.

## III. Analysis of irradiation creep - swelling interaction based on rate theory

### 1. Formula

(1) Irradiation creep strain due to climb-controlled glide process

The I-creep model proposed by Gittus[10] was applied to the calculation of swelling dependent-term. This model assumes a sequential climb and glide motion of dislocations. Stress loading induces the pinned dislocations to go on gliding and bowing out until the applied stress is balanced by the dislocation line tension force. After the bowed dislocations climb over the pinned points, the deflection of dislocation line segment is released, thus starts to glide until reaching a balance between the applied stress and the line tension. According to formulas derived by Heald[11], the strain rate

($\dot{\varepsilon}_{CCG}$) by I-creep model is expressed in the form;

$$\dot{\varepsilon}_{CCG} = \frac{\sigma_s \sqrt{\pi \cdot \rho_d}}{2\mu b} \cdot b\nu \ , \qquad \text{------- (15)}$$

where climb distance was assumed to be a half of the dislocation spacing, i.e. ($\pi \cdot \rho_d$)$^{-1/2}$. The symbol $\sigma_s$ means the shear stress, $\rho_d$ the dislocation density, $\mu$ the shear modulus, b Burgers vector, and $\nu$ the climb velocity. The dislocation climb motion proceeds by the absorption of interstitial atoms under neutron irradiation. The climb velocity is given in the form;

$$b\nu = Z_I D_I C_I^0 - D_V (C_V^0 - C_V^e) \ . \qquad \text{-------- (16)}$$

The symbol $C_x^0$ represents the concentration of interstitials (x=I) and vacancies (x=V), $C_V^e$ the thermal equilibrium concentration of vacancies, $Z_I$ the dislocation bias factor for interstitials, and $D_x$ the diffusion coefficient of interstitials (x=I) and vacancies (x=V). Multiplying shear stress ($\sigma_s$) by a Taylor factor (M) can provide for a tensile stress ($\sigma$), being the same as equivalent stress;

$$\sigma = M \cdot \sigma_s . \qquad \text{-------- (17)}$$

The strain rate provided by climb-controlled glide can be given by inserting equations (16) and (17) into equation (15):

$$\dot{\varepsilon}_{CCG} = \frac{\sigma \sqrt{\pi \cdot \rho_d}}{2\mu b M} \cdot \left\{ Z_I D_I C_I^0 - D_V (C_V^0 - C_V^e) \right\}. \qquad \text{------ (18)}$$

Equation (18) can be consequently transformed to the formulas,

$$\dot{\varepsilon}_{CCG} = \frac{\sqrt{\rho_d} \cdot \sigma}{\alpha \mu b} \left\{ \ Z_I D_I C_I^0 - D_V (C_V^0 - C_V^e) \right\} , \qquad \text{------- (19)}$$

$$\alpha = \frac{2M}{\sqrt{\pi}} \quad . \qquad \text{------ (20)}$$

The Taylor factor M was considered to be about 3 [18], thus inserting it into equation (20) gives a value of 3.4 for the coefficient $\alpha$.

(2) Volumetric swelling

The change in void radius ($r_c$) is given by the differential equation

$$\dot{r}_c = \left\{ D_V (C_V^0 - C_V^e) - D_I C_I^0 \right\} \ / \ r_c , \qquad \text{------- (21)}$$

as described by Mansur.[19] Volumetric swelling (S) is calculated by summation over all j-classes of voids as

$$S = \frac{4}{3}\pi \sum_j \rho_{cj} r_{cj}^{\ 3} \ , \qquad \text{------ (22)}$$

$$dS = 4\pi \sum_j \rho_{cj} r_{cj}^2 dr_{cj} + \frac{4}{3}\pi \sum_j d\rho_{cj} r_{cj}^3 \, . \qquad \text{------- (23)}$$

The symbol $\rho_{cj}$ represents the j-class void number density, and $r_{cj}$ the j-class void radius. The voids nucleated at j-th time step are classified into j-class voids. In the calculation, each time step produces a certain number of void nucleation, and such voids grow in the next time step. In this formula, increasing of both the void number density and void radius is taken into account for the calculation of volumetric swelling.

If the void number density is constant as $\rho_c$, volumetric swelling rate ($\dot{S}$) can be simply expressed in the form,

$$\dot{S} = 4\pi\rho_c r_c^2 \dot{r}_c = 4\pi\rho_c r_c \left\{ D_V (C_V^0 - C_V^e) - D_I C_I^0 \right\} . \qquad \text{-------(24)}$$

(3) Irradiation creep – swelling coupling coefficient D

The coefficient D should be defined as the ratio of the creep rate caused by climb-controlled-glide process to volumetric swelling rate divided by applied stress according to equation (1) :

$$D = \frac{\dot{\varepsilon}_{\mathrm{CCG}}}{\dot{S} \cdot \sigma} . \qquad \text{------ (25)}$$

The point defect concentrations under irradiation can be derived by solving the simultaneous differential equations[19)]

$$\dot{C}_I = p - k_I^2 D_I C_I^0 - R C_I^0 C_V^0 , \qquad \text{-----(26)}$$

$$\dot{C}_V = p - k_V^2 D_V C_V^0 - R C_I^0 C_V^0 . \qquad \text{----- (27)}$$

The symbol R represents the recombination rate, p the production rate of point defects, $k_x^2$ sink strength for interstitial (x=I) and vacancy (x=V). In the case of steady state condition ($\dot{C}_x = 0$, x=I, V), the point defect concentrations can be expressed in the form

$$C_{\chi}^{0} = \frac{p \cdot F(\eta)}{D_x \cdot k_x^2} \quad , \qquad \text{------ (28)}$$

$$F(\eta) = \frac{2}{\eta}\left\{(1+\eta)^{1/2} - 1\right\} \ , \qquad \text{------ (29)}$$

$$\eta = \frac{4R \cdot P}{D_V D_I k_I^2 k_V^2} \, . \qquad \text{------ (30)}$$

Under an assumption of constant void number density, applying swelling rate equation (24) together with equations (19) and (28) leads to a description of direct relationship between the climb-controlled-glide creep rate and volumetric swelling rate, neglecting the thermal equilibrium concentration of vacancies:

$$\dot{\varepsilon}_{CCG} = \frac{\sqrt{\rho_d} \cdot \sigma}{4\pi \, r_c \rho_c \alpha \mu b} \cdot \frac{Z_I k_V^2 - k_I^2}{k_I^2 - k_V^2} \cdot \dot{S} \quad . \qquad \text{------ (31)}$$

The coefficient D is defined as described in equation (25), and is consequently expressed by the formula

$$D = \frac{\sqrt{\rho_d}}{4\pi \, r_c \rho_c \alpha \mu b} \cdot \frac{Z_I k_V^2 - k_I^2}{k_I^2 - k_V^2} \, . \qquad \text{------- (32)}$$

In a case where only dislocations and voids act as point defects sinks, the total sink strength can be expressed in the form

$$k_I^2 = Z_I \rho_d + 4\pi r_c \rho_c , \qquad \text{------- (33)}$$

$$k_V^2 = \rho_d + 4\pi r_c \rho_c . \qquad \text{------- (34)}$$

Inserting equations (33) and (34) into (32) reveals that the coefficient D is constant:

$$D = \frac{1}{\alpha \mu b \sqrt{\rho_d}} \ . \qquad \text{------- (35)}$$

The strain rate ($\dot{\varepsilon}_{CCG}$) is hence proportional to volumetric swelling rate ($\dot{S}$), which is certainly the model proposed by J.H.Gittus and formulated by P.T.Heald.[11)]

However,, the irradiation test results presented in **Fig.4**, **Fig.5** and **Fig.10** reveal the fact that the coefficient D is not constant. The coefficient D is large at the onset of swelling and declines asymptotically to a constant value with increasing swelling. In steels under neutron irradiation, precipitates are known to act as point defect sinks. When the precipitates are taken in account as a neutral sink for point defects, the total sink strength can be expressed as

$$k_I^2 = Z_I \rho_d + 4\pi r_c \rho_c + S_p , \qquad \text{------- (36)}$$

$$k_V^2 = \rho_d + 4\pi r_c \rho_c + S_P . \qquad \text{------- (37)}$$

The symbol $S_p$ represents the precipitate sink strength. Inserting these equations into equation (32) gives the formula;

$$D = \frac{1}{\alpha\mu b\sqrt{\rho_d}} \cdot \left(1 + \frac{S_p}{4\pi r_c \rho_c}\right) \cdot \qquad \text{------- (38)}$$

The progression of volumetric swelling (S) corresponds to an increase of the denominator $4\pi r_c\rho_c$ of the equation (38). This equation hence suggests that the progression of volumetric swelling (S) leads the coefficient D to decrease asymptotically to a constant value of $1/\alpha\mu b\sqrt{\rho_d}$. We must keep in mind that equation (38) is valid only when the void number density is constant, because equation (24) was applied as volumetric swelling rate in this formulation.

**2. Numerical calculation**

The differential equations (26) and (27) are solved simultaneously to derive the steady state point defect concentrations ($C^0_x$, x=I, V), which are inserted into equations (19) and (23) to derive the creep strain rate ($\dot{\varepsilon}_{CCG}$) and the volumetric swelling rate ($\dot{S}$), respectively. I must emphasize that increasing both void number density and void radius should be taken into account by using equation (23) for swelling rate calculation. The coefficient D is then evaluated by substituting the strain rate ($\dot{\varepsilon}_{CCG}$) and the volumetric swelling rate ($\dot{S}$) derived into equation (25). The creep strain ($\varepsilon_{CCG}$) and the volumetric swelling (S) were derived by summing up the instantaneous creep rate ($d\varepsilon_{CCG}$) and swelling rate (dS) multiplied by neutron dose increment ($d\phi_t$).

TEM observation results of the neutron-irradiated tubes are presented in **Fig.11**, which revealed that precipitates with a blocky shape ($M_6C$ carbides) were formed at an

Fig.11

irradiation temperature ($T_{irr}$) of 678 K, and precipitates with both a blocky shape and a rod-like shape (Laves phase) at $T_{irr}$=823 K. Both are typical incoherent precipitates, and some of voids are attached to precipitates. However, the fraction of the attached voids is much smaller than matrix voids, judging from the detail image processing of photographs. Therefore, the vacancies flowing to voids attached to precipitates are presumed not to contribute the progression of void swelling. In this calculation, only matrix voids were taken into account and precipitate were regarded as the neutral sink for point defects. Based on above consideration, the sink strength of the precipitates ($S_p$) was estimated as a neutral sink according to the general expression[20)]

$$S_p = 4\pi r_p \rho_p + 4\pi \rho_{rod} \cdot L \cdot \ln(2L/N) . \qquad \text{----------(39)}$$

The symbol $r_p$ represents the average radius of blocky precipitates, $\rho_p$ the number density of the blocky precipitates, $\rho_{rod}$ the number density of the rod-like precipitates, and L and N are the average length of the longest axis and shortest axis of the rod-like precipitates, respectively. The ratio of L to N was assumed to be 5.0 from TEM observation shown in **Fig.11**. The simple formula of sink strength, case(1) and case(2), increasing linearly with neutron dose and having different incubation dose for precipitation was incorporated into the calculation, as shown in **Fig.12**. The slopes of the lines were appropriately selected so that these lines pass through the data experimentally evaluated at 139 dpa and 823 K as well as 206 dpa and 678 K, which are summarized in **Table 3**.

Fig.12

Table 3

The parameters used in the calculation are summarized in **Table 4**. The dislocation line density ($\rho_d$) in the calculation was determined from TEM observation of

Table 4

pressurized tubes made of PNC316 55MK heat after neutron irradiation. In the calculation, swelling was set to start at a dose of 70 dpa based on the diametral measurement results presented in **Fig.1**. Two types of void number densities ($\rho_c$) were applied: a linear increase of $\rho_c$ for neutron dose exceeding 70 dpa, and a constant $\rho_c$ for dose exceeding 70 dpa as shown in **Fig. 13**. The slopes of 2.5 x $10^{19}$ /$m^3$/dpa for 678 K and 2.0 x $10^{18}$ /$m^3$/dpa for 823 K were selected so as to pass through the measured void number densities. The value of dislocation bias factor ($Z_I$) for interstitial atoms was appropriately selected to make the value of volumetric swelling calculated consistent with the one evaluated by density measurements shown in **Table 3**.

Fig.13

The fitted curve and the measured swelling data are shown in **Fig.14**, where the selected values of dislocation bias factor ($Z_I$) for interstitial atoms are shown at each irradiation temperature and for each calculation parameter. The values of void radius calculated were 19 nm for the case of the linear increase of $\rho_c$, irradiation temperature ($T_{irr}$)=678K and neutron dose ($\phi_t$)=206 dpa, 35nm for that of the linear increase of $\rho_c$, $T_{irr}$=823K and neutron dose ($\phi_t$)=139 dpa, 22nm for the case of the constant $\rho_c$, irradiation temperature ($T_{irr}$)=678 K and neutron dose ($\phi t$)=206 dpa, and 40nm for that of the constant $\rho_c$, $T_{irr}$=823 K and neutron dose ($\phi t$)=139 dpa. These data reasonably agree with the TEM observation data presented in **Table 3**. The swelling rate derived in this calculation is suppressed to be less than about 0.15 %/dpa for 678 K and about 0.1%/dpa for 823 K. Therefore, void nucleation and growth coexisted within this swelling transient region. An adoption of the case of the linear increase of void number density seems to be preferable, rather than the case of constant $\rho_c$. In this study, however, both cases of trend for void number density are incorporated to derive the irradiation creep-swelling coupling coefficient D by equation (25).

Fig.14

## IV. Results and Discussions

### 1. Rate theory based analyses

The swelling-dependent term of irradiation creep was evaluated by subtracting the swelling-independent term from the total creep strain. At temperatures of 678 K and 823 K, thermal creep strain is quite small and was neglected in this study.[21] The swelling-independent term was evaluated by multiplying a creep compliance ($B_o$) by neutron dose ($\phi_t$). The creep compliance ($B_o$) used for the evaluation is $8.4 \times 10^{-7}$ ($dpa^{-1}$ $MPa^{-1}$) at 678 K and $4.1 \times 10^{-7}$ ($dpa^{-1}$ $MPa^{-1}$) at 823 K, which is shown in **Fig.3**. **Fig. 15** shows the calculated and experimentally evaluated strains at a temperature ($T_{irr}$) of 678 K. The values of 1.41 and 1.18 were selected for the coefficient $\alpha$ to minimize the standard deviation between the experimental data and the calculated values at a hoop stress of 100 MPa with precipitate sink strength of case (2). **Fig.16** shows results of calculation and experiment in the case of 823 K. The values of 6.8 and 3.8 were chosen for the coefficient $\alpha$ using the least square method for the calculated results at a hoop stress of 100 MPa with precipitate sink strength of case (2). The theoretical value of 3.4 for the coefficient $\alpha$, as derivated in equation (20), is located within a variation of the selected ones (1.18, 1.41, 3.8, 6.8).

Fig.15

Fig.16

**Fig.17** shows the calculated results and the experimentally evaluated data for the coefficient D as a function of volumetric swelling. At a temperature of 823 K, the MOTA data with a 100 MPa hoop stress is not shown in **Fig.17**, because the coefficient D is obviously overestimated by a low estimate of swelling due to neglecting the stress enhanced swelling as shown in **Fig.2**. The calculated values are shown to decline with increasing swelling similar to the experimentally evaluated data., and both the

Fig.17

calculation and experimental evaluation are well consistent each other. It was also demonstrated that D coefficient estimated using the constant void number density, as shown by solid squares and circles in Fig.17, agreed with the derived ones by substituting void radius and number density, precipitate sink strength and dislocation density into equation (38).

The decline of D with increasing swelling can be interpreted by partitioning of point defects between sinks: dislocations, voids and precipitates. The point defect flux to each sink is presented in **Fig.18**, which is the calculated result with the irradiation temperature ($T_{irr}$) of 678K and either the precipitate sink strength of case (1) or without precipitate sink. In the calculation, the net flux of vacancies to voids (Fv) and precipitates (Fp) as well as the net flux of interstitial atoms to dislocations (Fd) were evaluated using the following equations as functions of the point defect concentrations:

Fig.18

$$Fv = 4\pi r_c \rho_c \cdot (D_V (C_v^0 - C_V^e) - D_I C_I^0) \quad , \qquad \text{----- (40)}$$

$$Fp = Sp \cdot (D_V (C_v^0 - C_V^e) - D_I C_I^0) \quad , \qquad \text{----- (41)}$$

$$Fd = Z_I D_I C_I^0 - D_V (C_V^0 - C_V^e) \quad . \qquad \text{----- (42)}$$

Interstitial atoms preferentially flow into dislocations due to the bias effect of interstitials towards dislocations. It should be noted that there is a certain correlation between the interstitial flux to dislocations (Fd) and the sum of vacancy fluxes to voids and precipitates. The flux of interstitials to dislocations (Fd) is proportional to the sum of vacancy fluxes to voids and precipitates (Fv+Fp) as seen in **Fig.18 (a)** and **(c)**. This means that the excess vacancies caused by the preferred absorption of interstitial atoms

in dislocations are partitioned to both neutral sinks—void and precipitate sink. Evolution of swelling means that the void sink strength becomes larger relative to the precipitate sink, so that fraction of the excess vacancy flow to the voids gradually increases. This increase in void sink strength results in the increase of Fv and consequently leads to the decline of the Fd to Fv ratio. **Fig.18(e)** reveals that the Fd to Fv ratio declines with neutron dose and asymptotically approaches a constant value in the same way as the coefficient D when the precipitate sink is incorporated in the calculation. It can be said that this precipitate sink induces an unbalanced partitioning of the excess vacancies between voids and precipitates. On the other hand, the Fd to Fv ratio is constant when the precipitate sink is not considered in the calculation (**Fig.18(f)**), where the excess vacancies are totally absorbed by voids. The coefficient D is proportional to the Fd to Fv ratio because the strain rate ($\dot{\varepsilon}_{CCG}$) and swelling rate ($\dot{S}$) are proportional to Fd and Fv, respectively, as described in equations(19) and (23). Hence, the decline of the coefficient D can be interpreted in the same way as the case of the Fd to Fv ratio. The presence of a precipitate sink could upset the proportionality of the net interstitial flux into dislocations to the net vacancy flux into the voids and result in the decline of the coefficient D.

**2. Comparison with Woo's model**

Woo and Garner reported an explanation of the decrease of coefficient D with increasing swelling based on the anisotropic to isotropic transition of dislocation microstructure.[22] They assume that an anisotropic dislocation microstructure should evolve in the pressurized tubes because of stress induced preferred absorption of interstitial atoms in the dislocations with Burgers vector parallel to the stress-loading

direction, and it should become more isotropic as the void microstructure evolves. This anisotropic to isotropic transition of dislocation microstructure is believed to decrease irradiation creep strain rate, and hence the coefficient D with increasing swelling, since the anisotropic dislocation microstructure enhances irradiation creep due to a higher fraction of dislocations contributing the deformation. The formation of an anisotropic dislocation microstructure and the anisotropic to isotropic transition of dislocation microstructure might be possible, however has not yet been shown to be generally the case. Therefore, some other mechanisms might be constructive for interpreting the decline of D with increasing swelling.

The model proposed in this paper focuses on the effect of the precipitate sink that is generally known to play an important role in radiation effects on swelling and some other mechanical properties of metallic materials. It should be noted that the model is fully based on the result of microstructural observations, i.e. an experimental basis. The calculated results based on this model were demonstrated to be quite consistent with experimental result. It can be said that the partitioning of point defects between sinks should be a robust model for explaining the decrease of D with increasing swelling.

## 3. Irradiation creep behavior in FFTF MFA-1

It was shown in previous papers[16,23] that void swelling was significantly enhanced in the fuel pin irradiation relative to material irradiation without fuel. This difference leads to the great problem that a swelling design equation constructed using material irradiation data may not be applicable to the prediction of fuel pin diameter increase. The origin of the enhanced void swelling in fuel pin irradiation has been synthetically

investigated[24-26], including effects such as the secondary stress induced by the swelling difference across the cladding thickness, and cladding temperature change during irradiation due to power decreases and assembly shuffling.

There is great concern whether the creep compliance $B_o$ and creep-swelling coupling coefficient D are affected by irradiation variables when the PNC316 cladding is irradiated as fuel pin cladding. Seran pointed out that the creep strains predicted using the material irradiation data base are roughly a factor of three lower than strains measured in fuel pins.[27] Comparing **Fig.3** for MOTA material irradiation and **Fig.9** for MFA-1 fuel pin irradiation indicates that $B_o$ for both irradiations is similar at approximately $1x10^{-6}$ [$MPa^{-1}$ $dpa^{-1}$]. The D values also exhibit a similar trend of decline with increasing swelling in both material and fuel pin irradiations, of which details were already discussed.

The fuel pin diameter change due to irradiation creep in MFA-1 fuel pins was calculated using $B_o$ and D derived from MOTA irradiation, of which temperature dependency was disregarded. The swelling equation constructed to predict reasonably the measured data was used in this calculation. In **Fig.6,** solid symbol means the measured swelling strain, and swelling equation was fitted to it. The open symbol means the predicted diameter change, and difference in open and solid symbols corresponds to the irradiation creep strain, which was calculated by summing up the incremental irradiation creep strain due to stress increase at intervals of incremental neutron dose. Comparing with the measured diameter change shown by the serrate like solid line, the calculated irradiation creep strain agrees well with measured one at the axial location of around 400 mm from core bottom, where diameter increase took peak and cladding is approximately 750 K and 100 dpa. At the upper core region

above temperature of 870 K, however, the measured creep strain is higher than calculated one, because the thermal creep strain was superimposed.

The swelling is very sensitive to the irradiation environmental variables; however, the irradiation creep rate appears to be proportional only to the applied stress and swelling rate. This is the result of a physical process of the irradiation creep mechanism. When we consider the $B_o$ term in terms of a SIPA mechanism, the creep strain induced by dislocation climb motion is dominated by the physical interaction between interstitial atoms and dislocations under the applied stress. In addition, the creep-swelling interaction term D is based only on physical parameters: shear modulus, Burgers vector and dislocation density as shown in equation (35). Therefore, it can be said that $B_o$ and D values derived by material irradiation are possibly applicable to the prediction of the fuel pin diameter change.

## V. Conclusions

The interaction between irradiation creep and swelling was investigated by evaluating volumetric swelling and irradiation creep strain of PNC316 irradiated in MOTA as pressurized tube and MFA-1 as fuel pins at FFTF. A rate theory analysis was executed to interpret the irradiation creep–swelling interaction, and following results were obtained.

(1) The creep compliance, $B_o$, as well as irradiation creep–swelling coupling coefficient, D, were precisely derived for Monju fuel pin cladding PNC316 based on both integral and differential types of irradiation creep equations.

(2) It was revealed that coefficient D decreases and asymptotically approaches a constant value determined through the integral type of analysis as the volumetric

swelling progresses. The decline of the coefficient D with increasing swelling was interpreted as resulting from the partitioning of point defects between dislocations, voids and precipitates. The constructed robust model predicted that presence of a precipitate sink upset the proportionality of the net interstitial flux into dislocations to the net vacancy flux into the void sink under sequential climb-controlled glide process of dislocation.

(3) It was demonstrated that $B_o$ and D coefficients derived by material irradiation are applicable for predicting the irradiation creep deformation in the fuel pins, although it was known that the swelling behavior is totally different in material irradiation and fuel pin irradiation.

**Acknowledgements**

We are pleased to thank to staffs of Pacific Northwest National Laboratory (former Westinghouse Hanford Company) for their cooperation with irradiation test in FFTF. We also wish to thank to members of Material Monitoring Section at Oarai R&D center of JAEA for carrying out post irradiation examination, and to Mr. M. Itoh of Nuclear Engineering System Inc. for his assistant of the analysis. In addition, the authors are pleased to thank Dr. L.K. Mansur, Dr. R.E. Stoller and Dr. F.A. Garner for their review of this manuscript.

**References**

1) K. Ehrlich, J.Nucl.Mater., 100 (1981)149-166.

2) J.P. Foster, W.G. Wolfer, A. Biancheria and A. Boitax, Proc. Conf. On Irradiation Embrittlement and Creep in Fuel Cladding and Core Components, BNES, London, 1973, p.273.

3) F.A. Garner, Irradiation Performance of Cladding and Structural Steels in Liquid Metal Reactors, Nuclear Materials, Part 1, Amaterial Science and Technology Volume 10A.

4) A. Uehira, S. Mizuta, S. Ukai and R.J. Puigh, J.Nucl.Mater., 283-287 (2000) 396.

5) M. Fujiwara, H. Uchida, S. Ohta, S. Yuhara, S. Tani and Y. Sato, Radiation-induced Changes in Microstructure: 13$^{th}$ Symposium Part I, ASTM-STP 955 (1987) 127.

6) I. Shibahara, S. Ukai, S. Onose and S. Shikakura, J.Nucl.Mater., 204 (1993)131.

7) P.T. Heald and M.V. Speight, Acta Metall. 23 (1975) 1389.

8) W.G.. Wolfer and M. Ashkin, J.Appl. Physics 47 (1976) 791.

9) R. Bullough and J.R. Willis, Philos. Mag. 31 (1975) 855.

10) J.H. Gittus, Philos. Mag., 25 (1972) 345.

11) P.T. Heald and J.E. Harbottle, J.Nucl.Mater., 67 (1977) 229.

12) A. Maillard, H. Touron, J.L. Seran and A. Chalony, Effectsif Radiation on Materials: 16th Int.Symp., STP 1175, Philadelphia: ASTM, 1993.

13) M.B. Toloczko and F.A. Garner, J.Nucl.Mater., 212-215 (1994) 509.

14) R.J. Puigh and R.E. Schenter, Effectsif Radiation on Materials: 12th Int.Symp., STP 870, pp.795, 1993.

15) S. Ukai and T. Uwaba, J.Nucl.Mater., 317(2003)93.

16) S. Ukai, T. Yoshitake, N. Akasaka, T. Donomae, K. Katsuyama, T. Mitsugi and T. Asaga, *American Nuclear Society Transactions*, 1998, pp.115.

17) T. Asaga, Advances in Nuclear Fuel Technology – Present and Future -, Atomic

Energy Society of Japan, (2001) pp.178-204, in Japanese

18) R.E. Stoller, S.J. Zinkle, J.Nucl.Mater. 283-287 (2000) 349.

18) L. K. Mansur, Philos. Mag., 39(4) (1979) 497.

19) L. K. Mansur, Nucl. Technol., 40(1978) 5.

20) A.D. Brailsford, L.K. Mansur, J.Nucl.Mater. 103&104 (1981)1403.

21) T. Itaki, S. Yuhara, I. Shibahara, H. Kubota, M. Itoh and S. Nomura, Materials for Nuclear Reactor Core Application, BNES, London, 1987, pp.203.

22) C.H. Woo, F.A. Garner and R.A. Holt, Effects of Radiation on Materials: 16th Int. Symp., STP 1175, Philadelphia: ASTM, pp.27-37 (1993).

23) S. Ukai, N. Akasaka, K. Hattori and S. Onose, Effects of Radiation on Materials: 18th Int. Symp., STP 1325, Philadelphia: ASTM, pp.808-821 (1999).

24) T. Uwaba and S. Ukai, J.Nucl.Mater., 305(2002)21-28.

25) N. Akasaka, I. Yamagata and S. Ukai, J.Nucl.Mater., 283-287(2000)169-173.

26) N. Akasaka, K. Hattori, S. Onose and S. Ukai, J.Nucl.Mater., 271&272(1999)370-375.

27) J.L. Seran, H. Touron, A. Maillard, P. Dubuisson, J.P. Hugot, E. Boulbin, P. Planchard and M. Pelletier, Effects of Radiation on Materials: 14th Int. Symp., STP 1046, Philadelphia: ASTM, pp.739-752 (1990).

**Figure captions**

Fig.1 Irradiation creep and swelling strains at 678 K conducted at FFTF/MOTA vehicle. Irradiation creep strain corresponds to equivalent strain.

Fig.2 Irradiation creep and swelling strains at 823 K conducted at FFTF/MOTA vehicle. Irradiation creep strain corresponds to equivalent strain.

Fig.3 The creep compliance Bo derived from FFTF/MOTA irradiation as a function of irradiation temperature.

Fig.4 Irradiation creep – swelling coupling coefficient D at 678 K as a function of volumetric swelling, which were derived from instantaneous irradiation creep rate and instantaneous volumetric swelling rate.

Fig.5 Irradiation creep–swelling coupling coefficient D at 823 K as a function of volumetric swelling, which were derived from instantaneous irradiation creep rate and instantaneous volumetric swelling rate.

Fig.6 Comparison of measured diametral change and predicted in PNC316 fuel pin (Pin No.186019). The predicted diametral change is total of the measured swelling strain and calculated irradiation creep strain using MOTA results.

Fig.7 Relation between diametral change and swelling strain in PNC316 fuel pins in MFA-1. The diametral change consists of swelling and irradiation creep strains.

Fig.8 Results of calculation on cladding equivalent stress vs. neutron dose at the axial core location of 320 mm from the core bottom of Pin No.186019 in MFA-1 (core length: 914 mm). The stress was induced by fission gases released from the fuel pellets.

Fig.9 Overall creep compliance $B_{ov}$ vs. instantaneous volumetric swelling rate, which was derived from Pin No.186019 in MFA-1.

Fig.10 Dependence of irradiation creep–swelling coupling coefficient D on volumetric swelling of PNC316 fuel cladding in MFA-1.

Fig.11 TEM observation results of neutron irradiated pressurized tube made of PNC316, (a) irradiation temperature(Tirr)=678K, hoop stress($\sigma_H$)=100MPa, neutron dose ($\phi$t)=206dpa, (b) Tirr=823K, $\sigma_H$=100MPa, $\phi$t=139dpa.

Fig.12 The precipitate sink strength at 678K and 873K in the calculation as a function of neutron dose.

Fig.13 Void number density as a function of neutron dose used for the calculation at 678 K and 823 K.

Fig.14 Swelling values evaluated by density measurements and that calculated by selecting a appropriate value of $Z_I$ for the calculation to be consistent with the measurements at 678K and 873K, (a) in the case that void number density increases linearly with neutron dose, (b) in the case that void number density is constant.

Fig.15 Irradiation creep strain due to climb-controlled glide process calculated by means of point defect kinetics theory at 678K and 100 MPa, (a) in the case that void number density increases linearly with neutron dose, (b) in the case that void number density is constant.

Fig.16 Irradiation creep strain due to climb-controlled glide process calculated by means of point defect kinetics theory at 823K and 100 MPa, (a) in the case that void number density increases linearly with neutron dose, (b) in the case that void number density is constant.

Fig.17 Irradiation creep-swelling coupling coefficient D calculated by means of point defect kinetics theory at (a) 678K and (b) 823K, comparing with MOTA and MFA-1 data.

Fig.18 Flux of point defects under irradiation calculated by defect kinetics theory (678K), net flux of interstitial to dislocation with precipitate case(1)(a), and without precipitate sink (b), net flux of vacancy to void and precipitate sinks with precipitate case(1) (c) and without precipitate sink (d), the ratio of net interstitial flux to dislocation per net vacancy flux to void with precipitate case(1) (e) and without precipitate sink(f).

Table 1　Chemicl composition and heat treatment of PNC316 55MK heat.

| Composition (mass%) | 55MK heat | 60MK heat | 60MS heat |
|---|---|---|---|
| C | 0.052 | 0.054 | 0.057 |
| Si | 0.82 | 0.78 | 0.79 |
| Mn | 1.83 | 1.72 | 1.85 |
| P | 0.028 | 0.028 | 0.026 |
| S | 0.009 | 0.003 | 0.002 |
| Ni | 13.84 | 13.45 | 13.72 |
| Cr | 16.52 | 16.22 | 16.33 |
| Mo | 2.49 | 2.35 | 2.54 |
| B | 0.0031 | 0.0039 | 0.0036 |
| N | 0.003 | 0.009 | 0.003 |
| Ti | 0.080 | 0.078 | 0.075 |
| Nb+Ta | 0.079 | 0.08 | 0.095 |
| V | 0.01 | 0.01 | 0.01 |
| Solution treatment | 1353 K x 2 min | 1353 K x 2 min | 1368K x 1min |
| Cold-work | 20.0% | 18.0% | 20.6% |

Table 2 Irradiation condition of pressurized and open tubes in FFTF/MOTA experiment.

| Temperature (K) [℃] | Hoop stress (MPa) | Exposed neutron dose (dpa) | Diameter change (%) | Density change (Vol.%) | FFTF cycle |
|---|---|---|---|---|---|
| 678 | 0 | 206 | 4.32 | 13.60 | 5 - 12 |
| [405] | 70 | 182 | 5.89 | 10.59 | 5 - 11 |
| | 100 | 206 | 9.10 | 15.07 | 5 - 12 |
| 713 | 0 | 82 | 0.14 | 0.50 | 5 - 11 |
| [440] | 70 | 79 | 0.58 | 0.45 | 5 - 11 |
| | 100 | 79 | 0.83 | 0.56 | 5 - 11 |
| 768 | 0 | 71 | -0.08 | -0.20 | 9 - 12 |
| [495] | 70 | 58 | 0.09 | -0.07 | 9 - 11 |
| | 100 | 71 | 0.25 | -0.11 | 9 - 12 |
| 823 | 0 | 139 | 0.23 | 1.40 | 9 - 12 |
| [550] | 70 | 117 | -0.12 | 0.60 | 9 - 11 |
| | 100 | 139 | 3.23 | 3.75 | 9 - 12 |
| 878 | 0 | 133 | -0.05 | 0.30 | 9 - 12 |
| [605] | 70 | 121 | 1.65 | 0.90 | 9 - 11 |
| | 100 | 133 | 3.85 | 2.38 | 9 - 12 |
| 943 | 0 | 104 | -0.12 | -0.30 | 10 - 12 |
| [670] | 70 | 104 | 7.14 | 0.07 | 10 - 12 |
| | 100 | 78 | 7.31 | — | 10 - 11 |

Table 3 Results of transmission electron microscope observation and density measurements of pressurized PNC316 55MK heat tubes neutron-irradiated in FFTF/MOTA.

| Items | Value | |
|---|---|---|
| Irradiation temperature, $T_{irr}$ | 678 K | 823 K |
| Neutron dose, $\phi_t$ | 206 dpa | 139 dpa |
| Hoop stress, $\sigma_h$ | 100 MPa | 100 MPa |
| - Dislocation density, $\rho_d$ | $3.5 \times 10^{14}$ $m^{-2}$ | $2.0 \times 10^{14}$ $m^{-2}$ |
| - Precipitates with particle-like shape | | |
| Average radius, $r_p$ | 11.8 nm | 46.8 nm |
| Number density, $\rho_p$ | $8.5 \times 10^{20}$ $m^{-3}$ | $2.8 \times 10^{20}$ $m^{-3}$ |
| - Precipitates with rod-like shape | | |
| Average length, $l_p$ | – | 136 nm |
| Number density, $\rho_p$ | – | $9.0 \times 10^{19}$ $m^{-3}$ |
| - Void | | |
| Average radius, $r_c$ | 16 nm | 52 nm |
| Number density, $\rho_c$ | $3.3 \times 10^{21}$ $m^{-3}$ | $1.4 \times 10^{20}$ $m^{-3}$ |

Table 4 Parameters used in the calculation.

| Parameter | Value | |
|---|---|---|
| Temperature , T [K] | 678 | 823 |
| Increasing rate of void number density (/$m^3$/dpa) | 2.5 x $10^{19}$ | 2.0 x $10^{18}$ |
| Diffusion coefficient of interstitial (! | | |
| $D_I$=8.0x$10^{-6}$ exp(-$E_I^m$/kT) [$m^2$ $s^{-1}$] | 1.54x$10^{-9}$ | 6.94x$10^{-9}$ |
| Diffusion coefficient of vacancy (! | | |
| $D_V$= 8.0x$10^{-5}$ xexp(-($E_V^m$+$E_V^f$)/kT) [$m^2$ $s^{-1}$] | 4.08x$10^{-27}$ | 3.42x$10^{-23}$ |
| Thermal equilibrium conc. of vacancy (*1) | | |
| $C_V^e$=exp(- $E_V^f$/kT) [$m^{-3}$] | 1.29x$10^{-12}$ | 1.60x$10^{-10}$ |
| Recombination factor | | |
| R=4π (4x$10^{-10}$)x ($D_I$+$D_v$) [$m^2$ $s^{-2}$] | 7.7x$10^{-18}$ | 3.5x$10^{-17}$ |
| Defects production rate (*2) | | |
| p=η$G_{dpa}$/Ω [$sec^{-1}$] | 4.95x$10^{22}$ | 4.95x$10^{22}$ |
| Shear Modulus (*3) | | |
| μ=E/2(1+ν) (GPa) | 65 | 59 |

(∗1) Migration energy of interstitial ($E_i^m$) = 0.5 eV
Migration energy of vacancy ($E_v^m$) = 1.4 eV
Formation energy of vacancy ($E_V^f$) = 1.6 eV
(∗2) Damage efficiency(η) =0.33
Damage rate ($G_{dpa}$) = 1.5x$10^{-6}$ dpa/sec
Atomic volume (Ω) = $10^{-29}$ $m^3$
(3) Poisson ratio (ν)= 0.3
Young's modulus (E) at 678K = 169GPa
Young's modulus (E) at 823K =and 154GPa

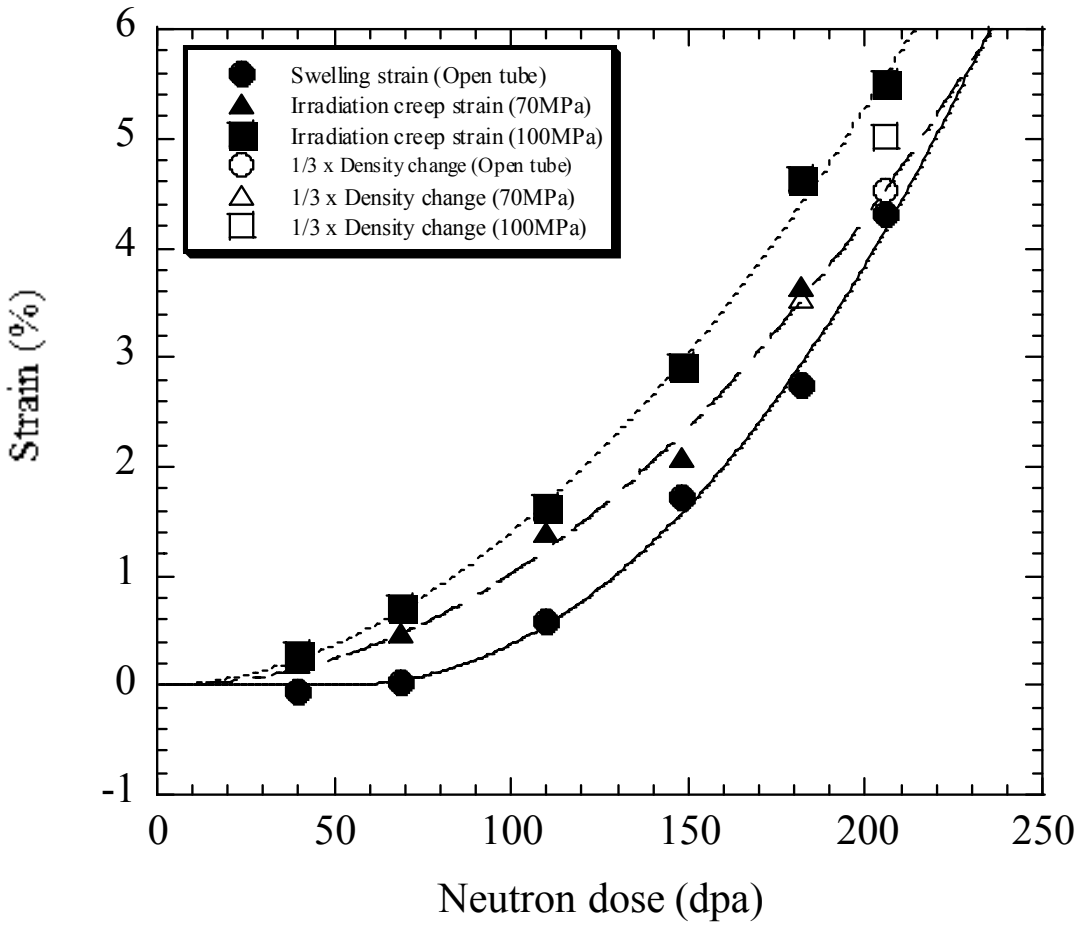


**Fig.1**

S.Ukai

Irradiation Creep - Swelling Interaction in Modified 316 Stainless Steel up to 200 dpa

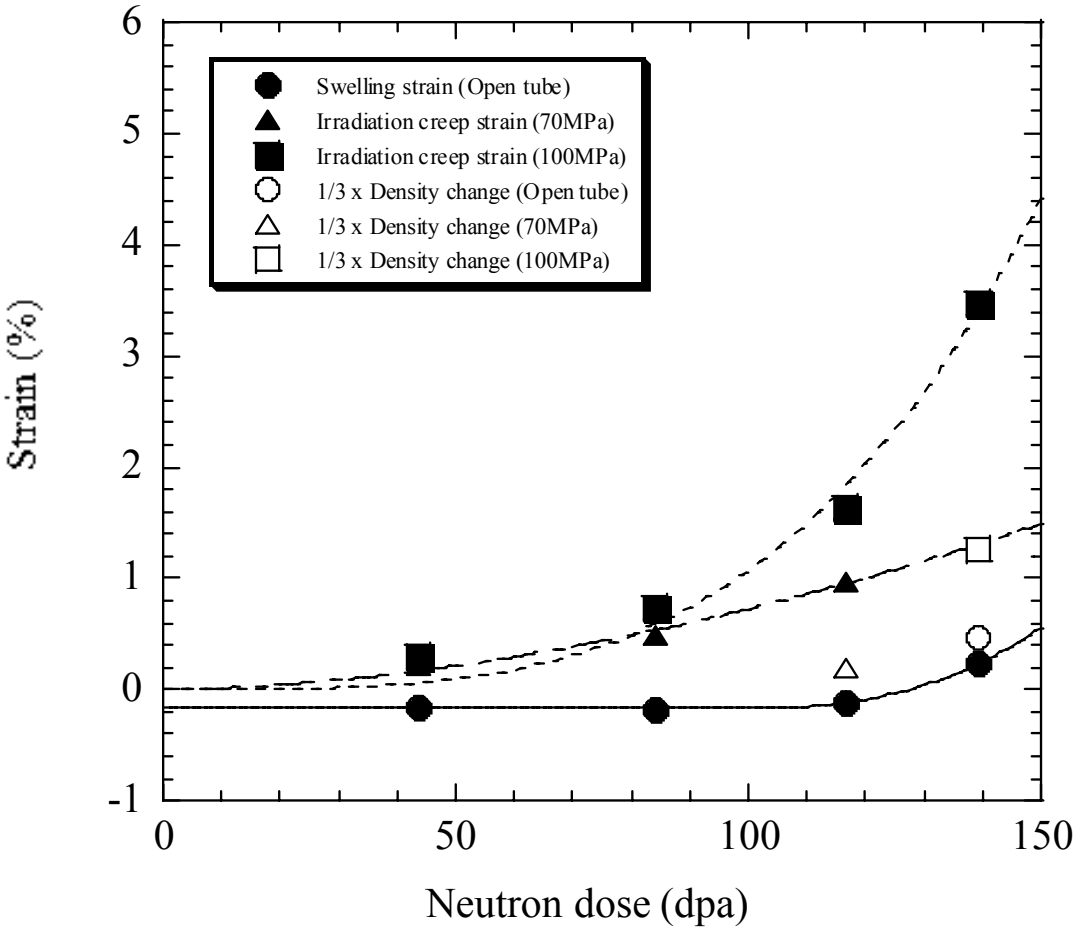


**Fig.2**

S.Ukai

Irradiation Creep - Swelling Interaction in Modified 316 Stainless Steel up to 200 dpa

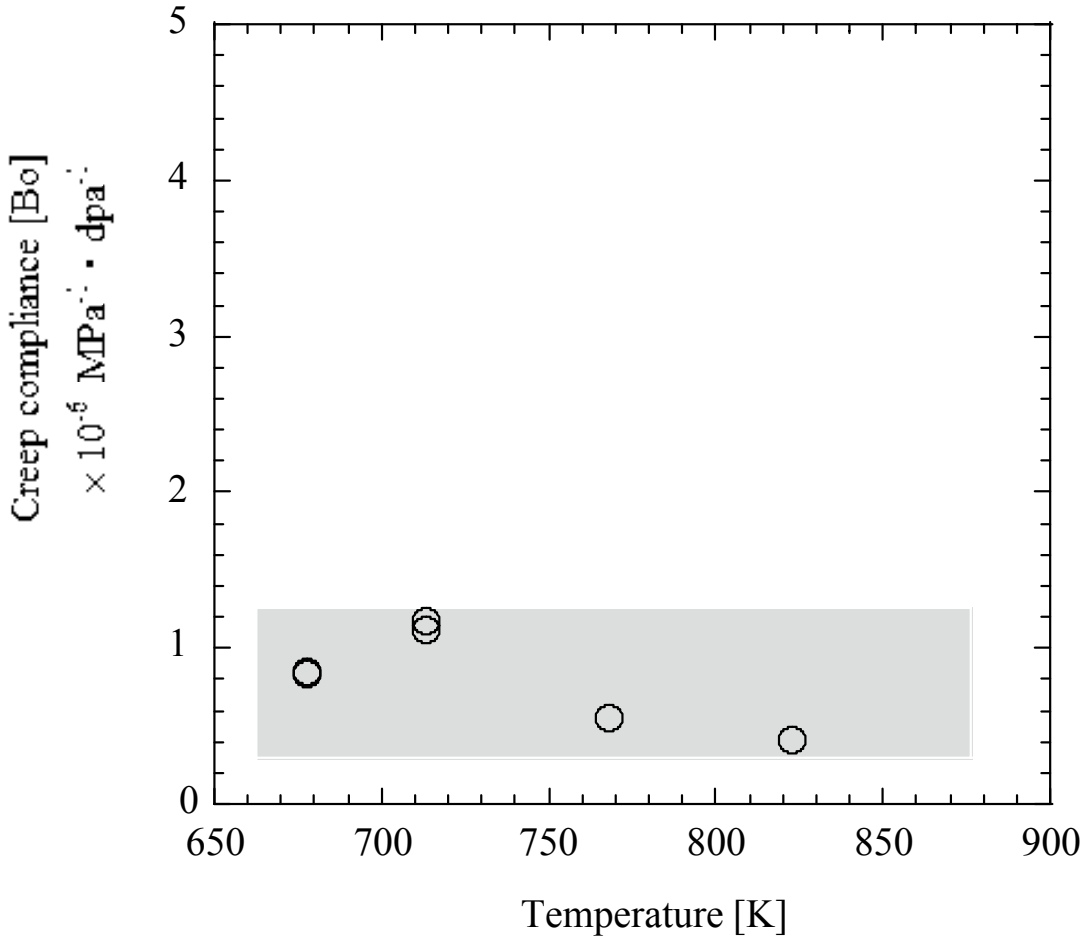


**Fig.3**

S.Ukai

Irradiation Creep - Swelling Interaction in Modified 316 Stainless Steel up to 200 dpa

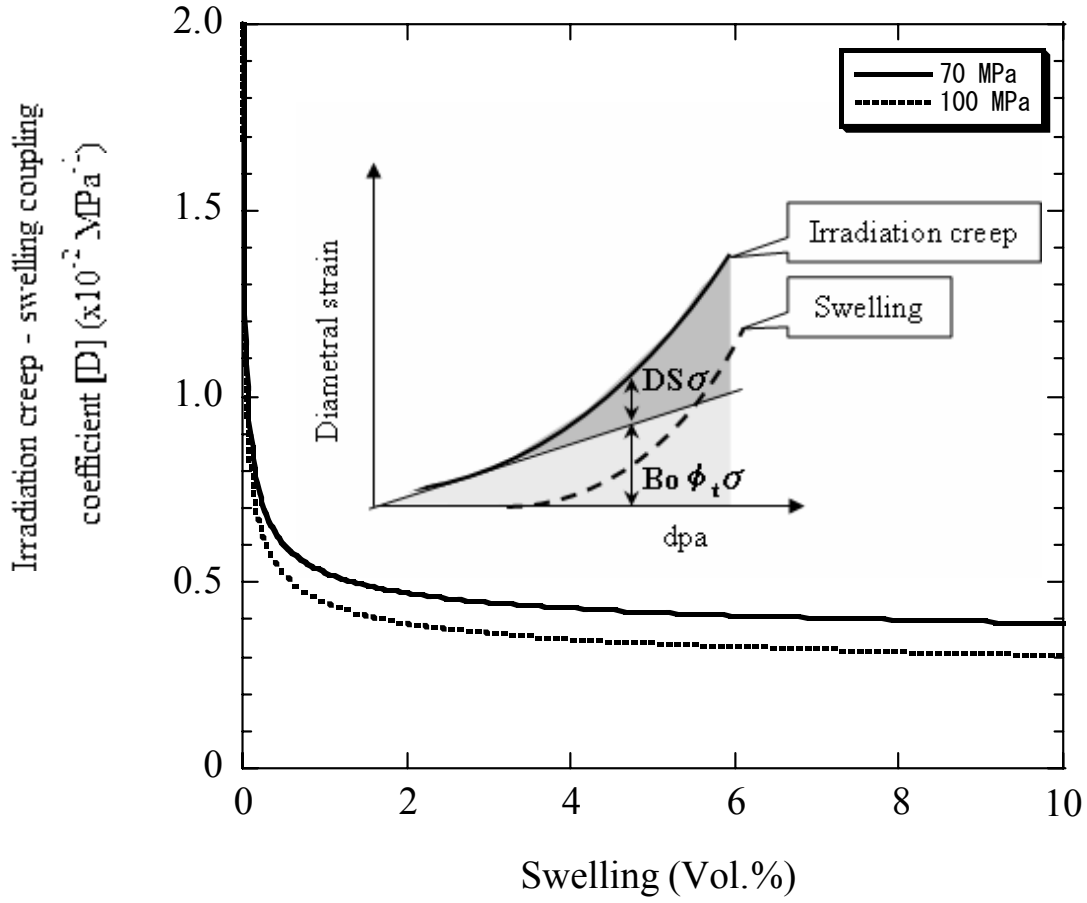


**Fig.4**

S.Ukai

Irradiation Creep - Swelling Interaction in Modified 316 Stainless Steel up to 200 dpa

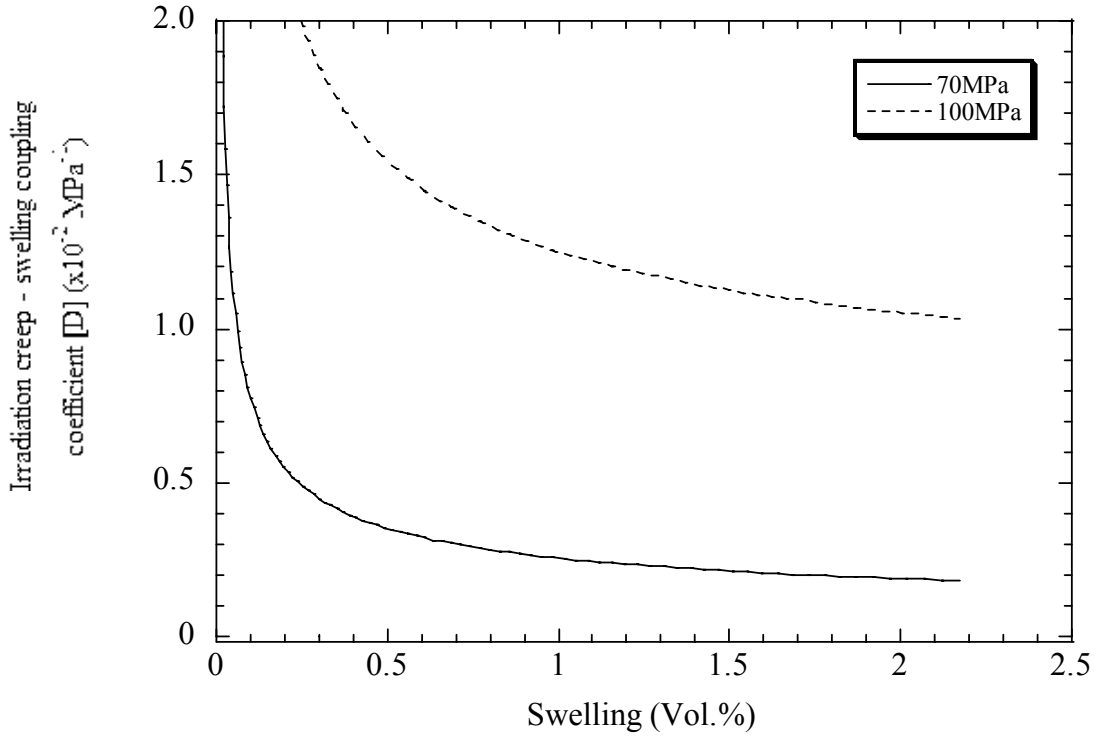


**Fig.5**

S.Ukai

Irradiation Creep - Swelling Interaction in Modified 316 Stainless Steel up to 200 dpa

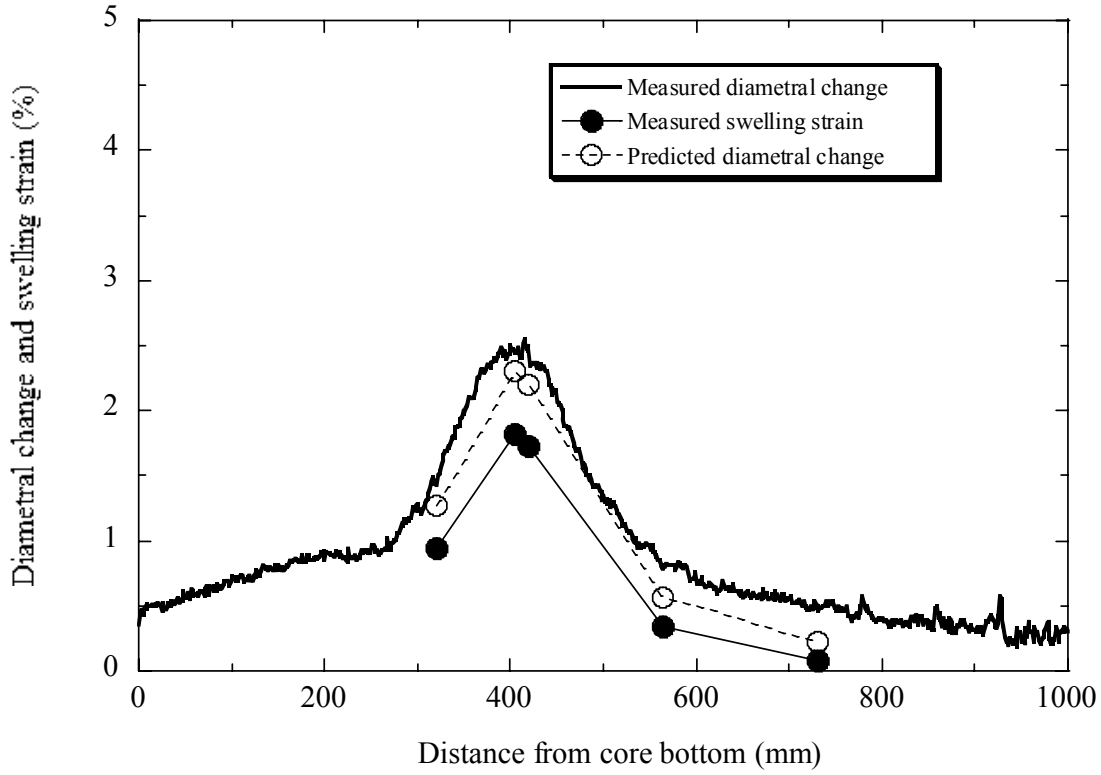


**Fig.6**

S.Ukai

Irradiation Creep - Swelling Interaction in Modified 316 Stainless Steel up to 200 dpa

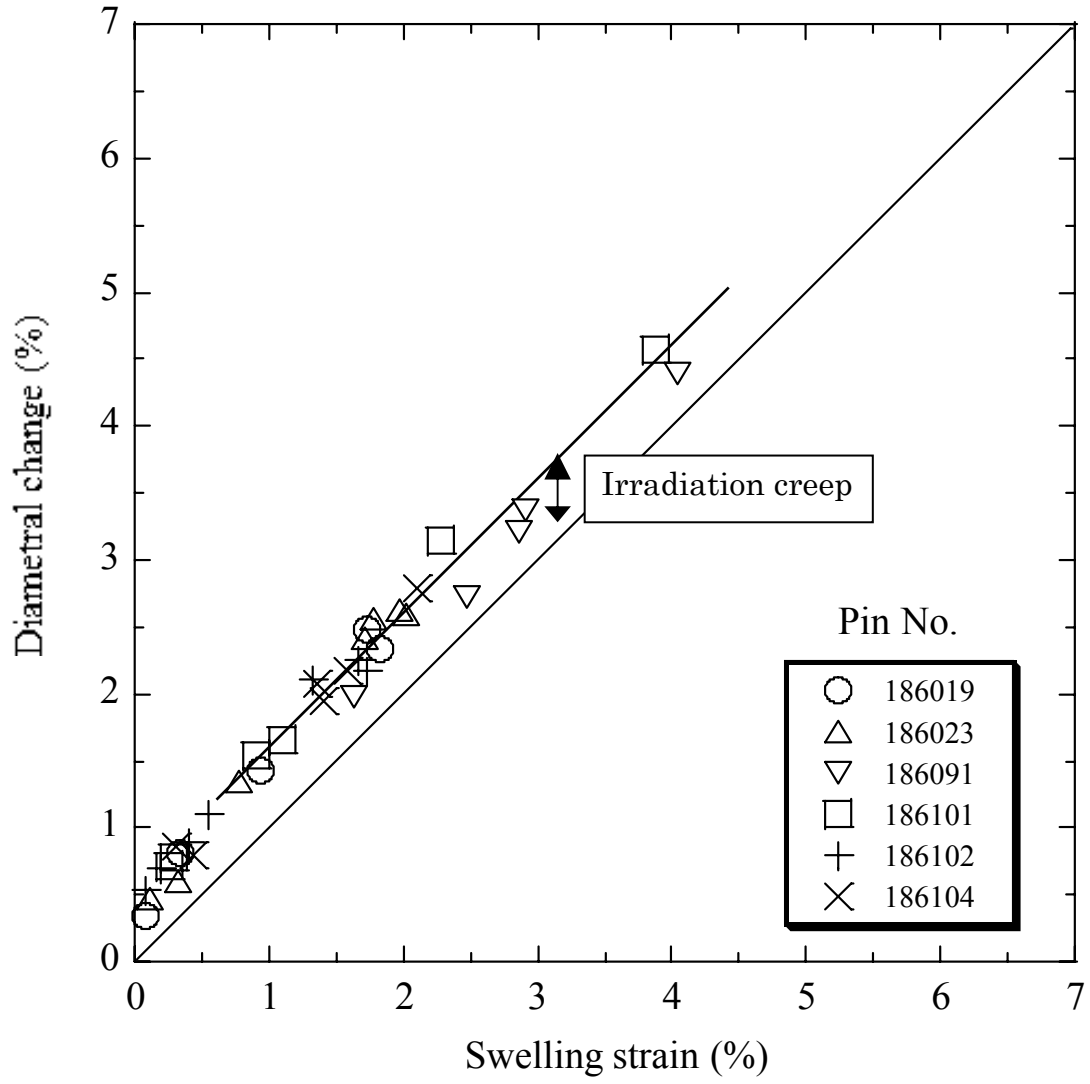


**Fig.7**

S.Ukai

Irradiation Creep - Swelling Interaction in Modified 316 Stainless Steel up to 200 dpa

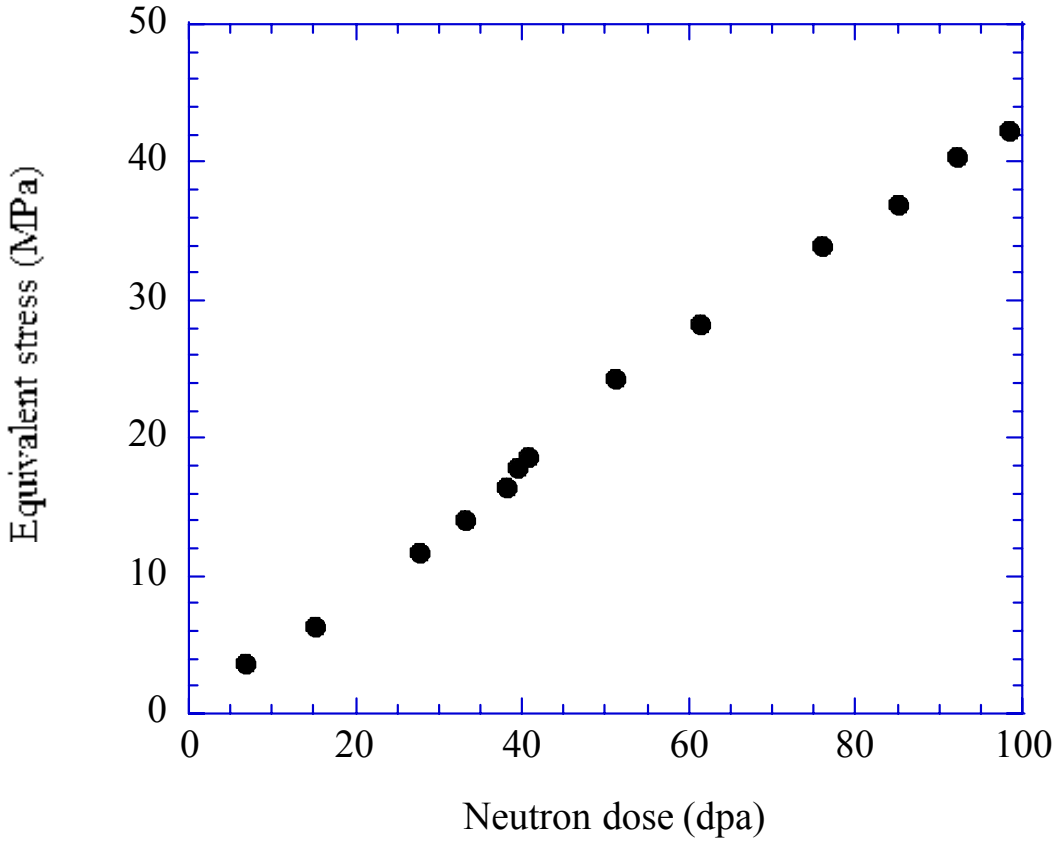


**Fig.8**

S.Ukai

Irradiation Creep - Swelling Interaction in Modified 316 Stainless Steel up to 200 dpa

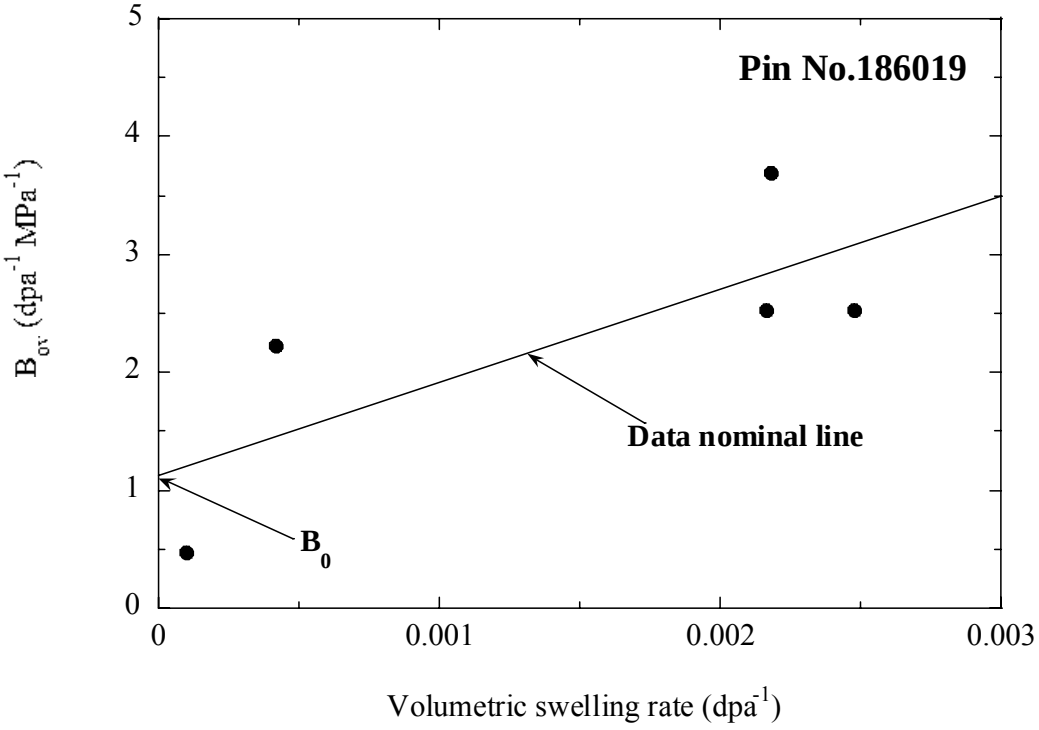


**Fig.9**

S.Ukai

Irradiation Creep - Swelling Interaction in Modified 316 Stainless Steel up to 200 dpa

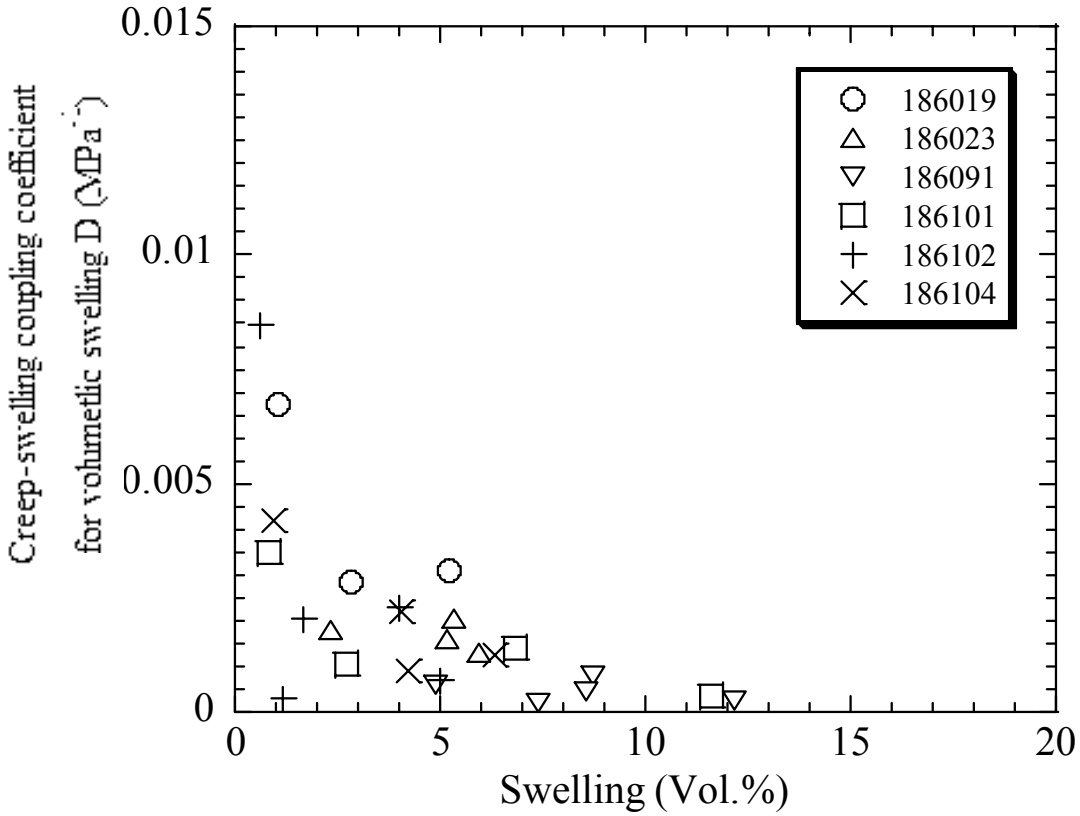


**Fig.10**

S.Ukai

Irradiation Creep - Swelling Interaction in Modified 316 Stainless Steel up to 200 dpa

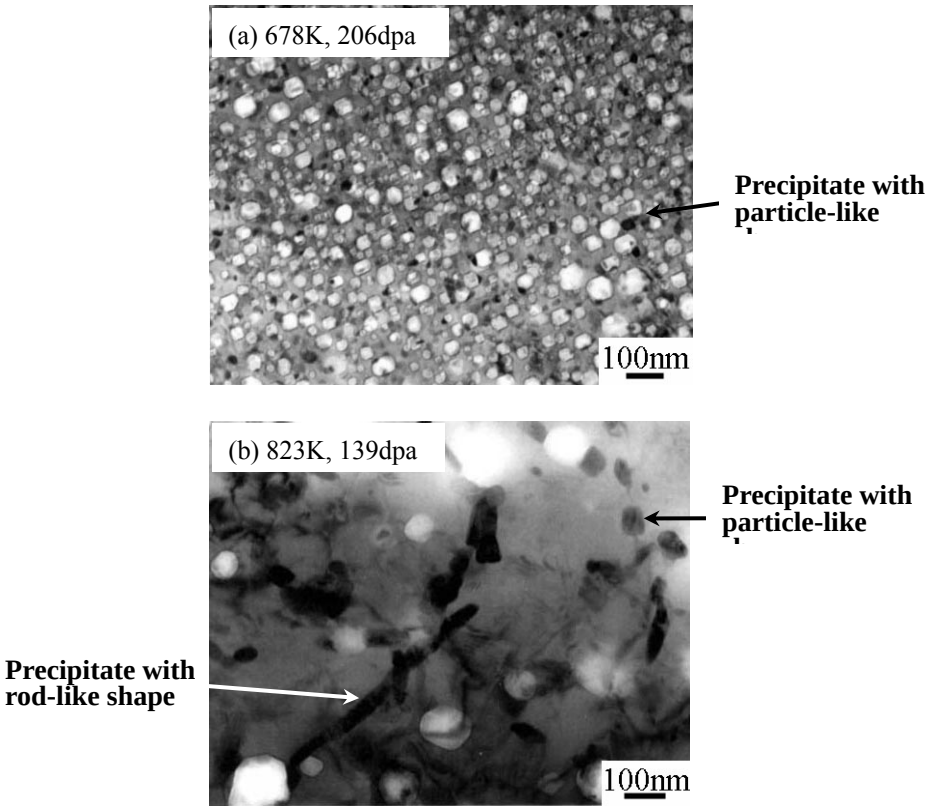


**Fig.11**

S.Ukai

Irradiation Creep - Swelling Interaction in Modified 316 Stainless Steel up to 200 dpa

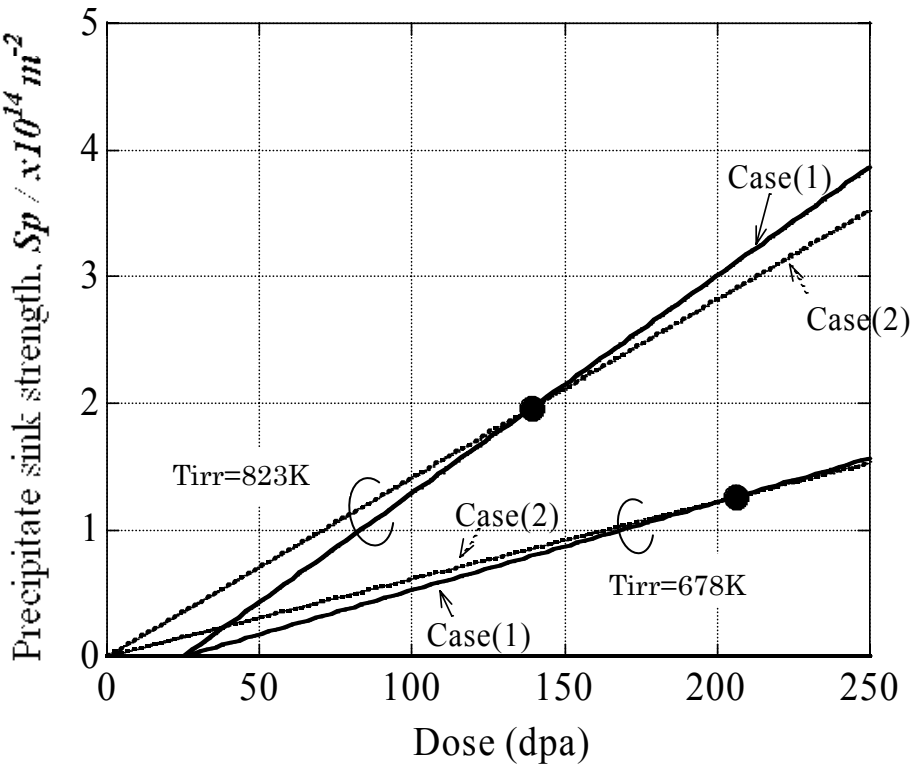


**Fig.12**

S.Ukai

Irradiation Creep - Swelling Interaction in Modified 316 Stainless Steel up to 200 dpa

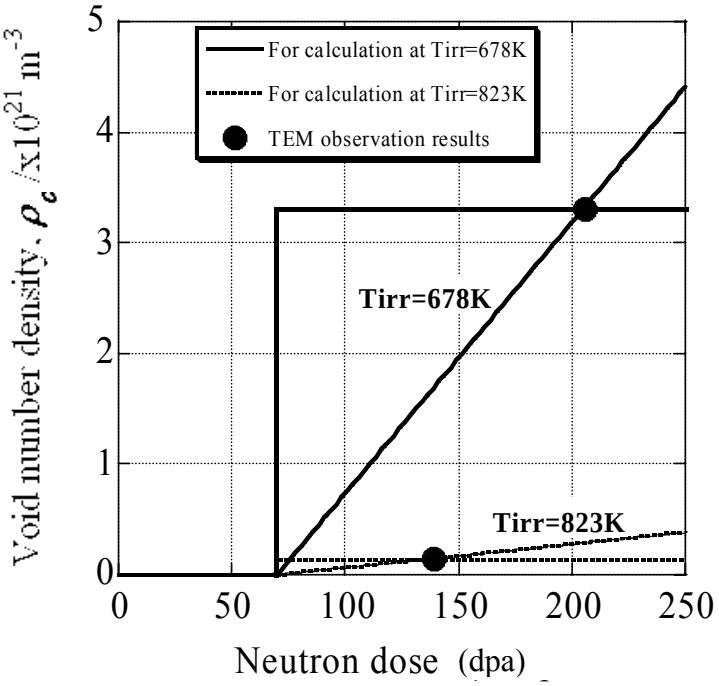


**Fig.13**

S.Ukai

Irradiation Creep - Swelling Interaction in Modified 316 Stainless Steel up to 200 dpa

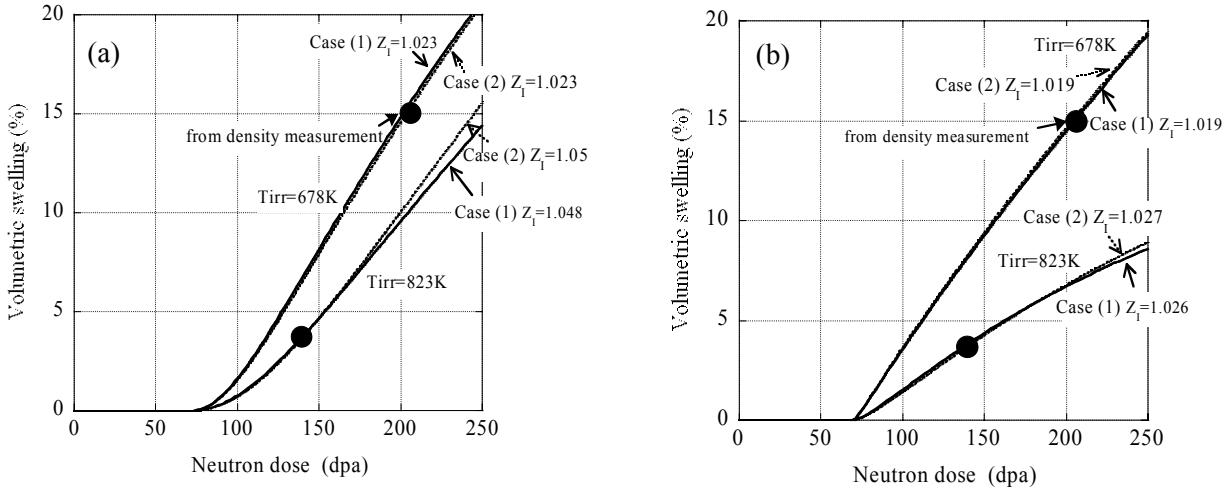


**Fig.14**

S.Ukai

Irradiation Creep - Swelling Interaction in Modified 316 Stainless Steel up to 200 dpa

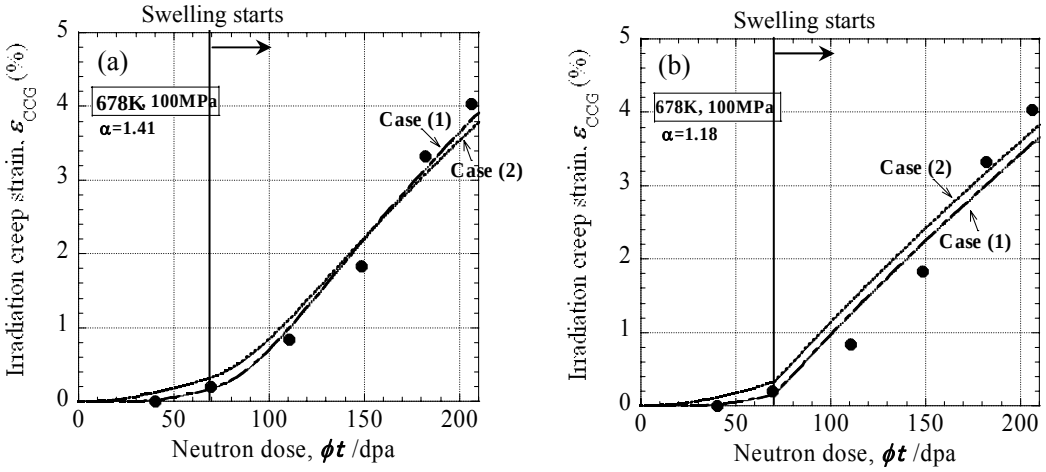


**Fig.15**

S.Ukai

Irradiation Creep - Swelling Interaction in Modified 316 Stainless Steel up to 200 dpa

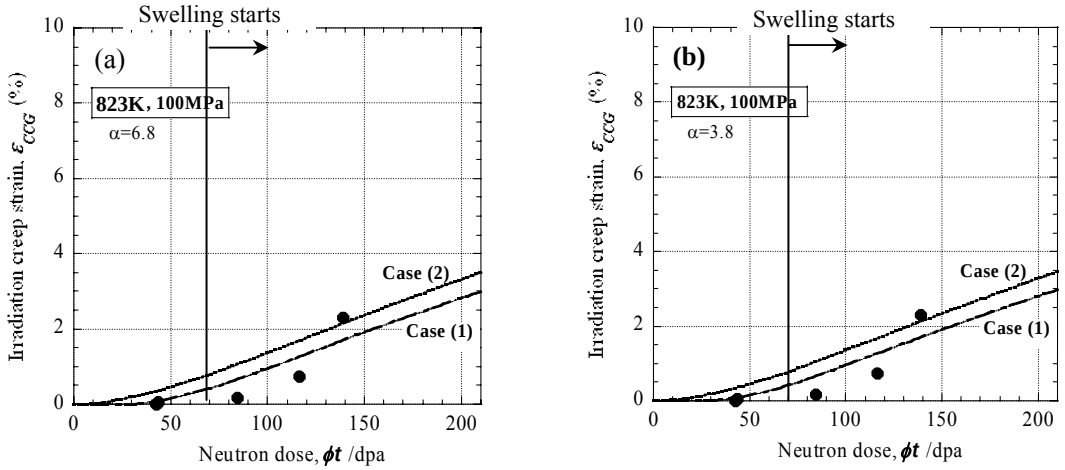


**Fig.16**

S.Ukai

Irradiation Creep - Swelling Interaction in Modified 316 Stainless Steel up to 200 dpa

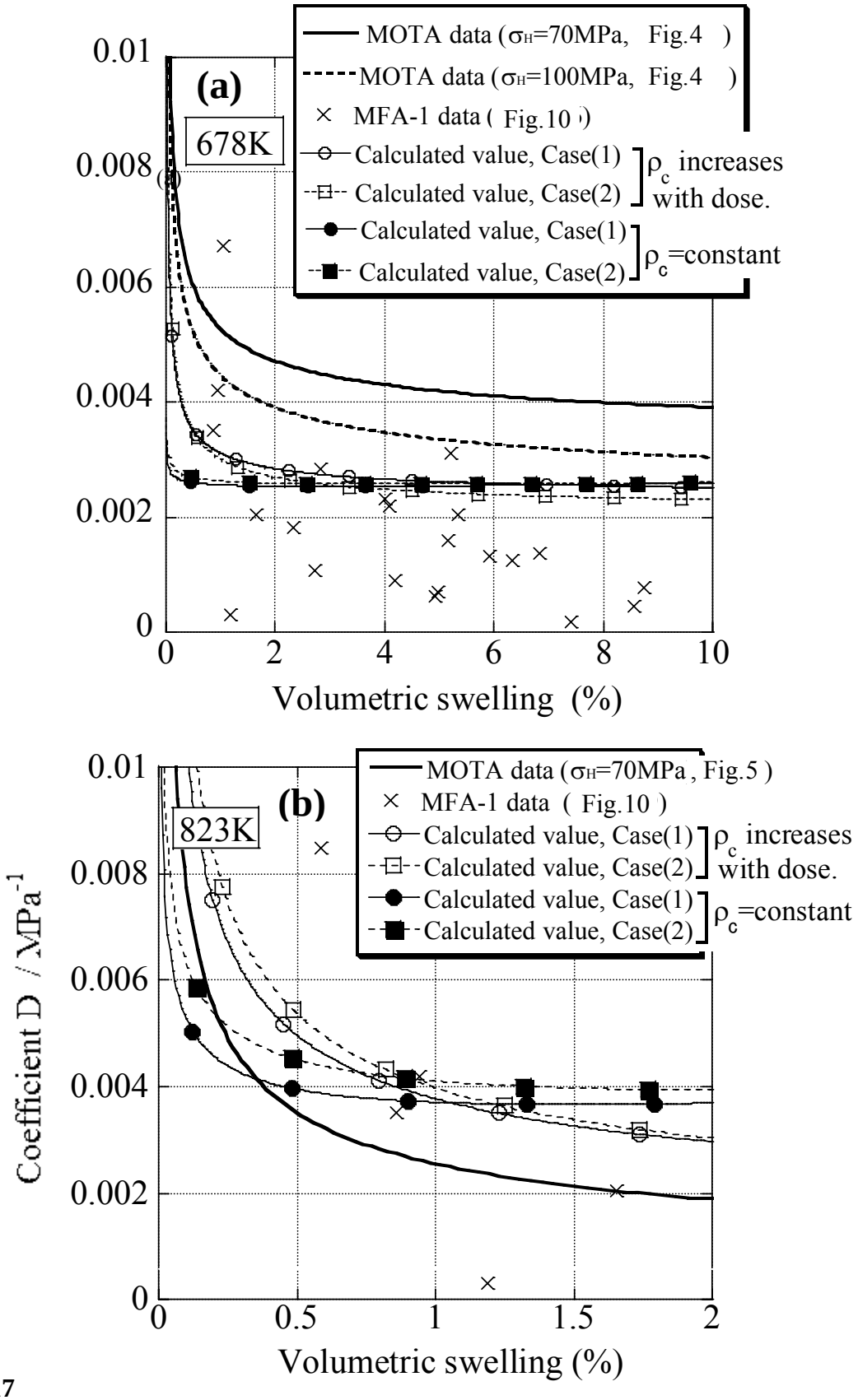


**Fig.17**

S.Ukai Irradiation Creep - Swelling Interaction in Modified 316 Stainless Steel up to 200 dpa

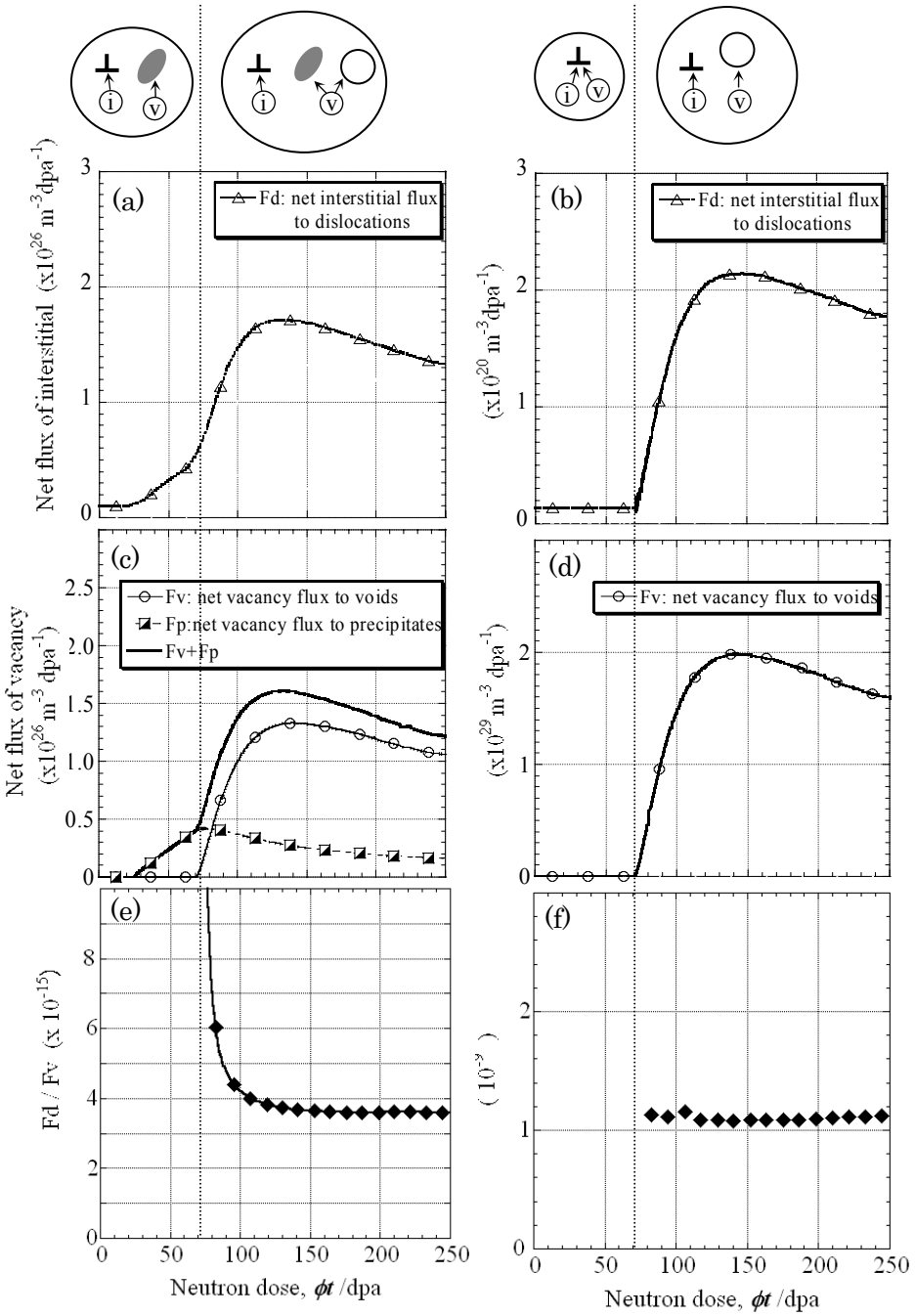


**Fig.18**

S.Ukai

Irradiation Creep - Swelling Interaction in Modified 316 Stainless Steel up to 200 dpa